



## Molecular properties affecting fast dissociation from the D<sub>2</sub> receptor

Gary Tresadern<sup>a,\*</sup>, Jose Manuel Bartolome<sup>b</sup>, Gregor J. Macdonald<sup>c</sup>, Xavier Langlois<sup>d,\*</sup>

<sup>a</sup> Research Informatics, Janssen Research & Development, Janssen-Cilag S.A., Calle Jarama 75, Poligono Industrial, Toledo 45007, Spain

<sup>b</sup> Neuroscience Medicinal Chemistry, Janssen Research & Development, Janssen-Cilag S.A., Calle Jarama 75, Poligono Industrial, Toledo 45007, Spain

<sup>c</sup> Neuroscience Medicinal Chemistry, Janssen Research & Development, Janssen Pharmaceutica NV, Turnhoutsweg 30, B-2340 Beerse, Belgium

<sup>d</sup> Neuroscience Discovery Biology, Janssen Research & Development, Janssen Pharmaceutica NV, Turnhoutsweg 30, B-2340 Beerse, Belgium

### ARTICLE INFO

#### Article history:

Received 17 November 2010

Revised 14 February 2011

Accepted 18 February 2011

Available online 26 February 2011

#### Keywords:

Fast dissociation

Dopamine D<sub>2</sub> receptor

D<sub>2</sub> antagonist

$k_{off}$

Multivariate analysis

Antipsychotic

Atypical

QSAR

Off-rate

Kinetics

Residence time

### ABSTRACT

Dopamine D<sub>2</sub> receptor antagonism is the foundation of antipsychotic treatment. Antipsychotic agents vary in how fast they dissociate from the D<sub>2</sub> receptors. It has been proposed that the liability to exhibit side effects such as extra pyramidal symptoms may be the result of a slow rate of dissociation. Compounds with a faster rate of dissociation, while still blocking efficiently the D<sub>2</sub> receptors, will subsequently respond better to physiological surges in dopamine transmission. Therefore, work in our laboratories has focussed on identifying fast dissociating and selective D<sub>2</sub> antagonists. Biological screening was performed to measure the affinity and extent of dissociation for a large dataset of over 1800 D<sub>2</sub> antagonists. Subsequent univariate and multivariate statistical analysis revealed the molecular properties which differentiate fast and slow dissociating compounds. It is shown that faster dissociating antagonists are less lipophilic and have lower molecular weight. There was a clear and expected inverse relationship with extent of dissociation and binding affinity with more potent compounds tending to be slower dissociating. However, within a range of comparable affinity both fast and slow dissociating compounds were identified. After de-correlating affinity and dissociation the analysis revealed the important descriptors.

© 2011 Elsevier Ltd. All rights reserved.

### 1. Introduction

Despite the potential new pathways involved in the cause of schizophrenia which have emerged in recent years,<sup>1</sup> the dopamine hypothesis<sup>2,3</sup> remains a cornerstone of schizophrenia research. This hypothesis is supported by several empirical observations. Dopamine enhancing drugs such as amphetamine induce psychotic-like symptoms, schizophrenic patients display increased levels of activity of the neurotransmitter dopamine,<sup>4</sup> and all known marketed antipsychotic drugs bind to the dopamine type 2 (D<sub>2</sub>) receptor and thereby are supposed to modulate dopamine hyperfunction.<sup>5,6</sup>

First generation or typical antipsychotics such as chlorpromazine and haloperidol (**1**) are highly effective in treating positive symptoms of schizophrenia such as hallucinations, delusions and incoherence but are less effective versus negative signs for example social withdrawal, apathy and anhedonia. Importantly, these medications can invoke side effects including Parkinson-like extra pyramidal (EPS) side effects and prolactin release through an

excessive blockade of the dopamine system in the basal ganglia<sup>7</sup> and the pituitary gland, respectively. In general, the second generation of antipsychotics, among which clozapine (**2**) is the most representative, show significantly lower levels of EPS and prolactin release.<sup>8,9</sup> The broad definition of atypicality includes antipsychotics exhibiting improved treatment of negative symptoms and action on other neurotransmitter receptors.<sup>10–12</sup> Although exhibiting less EPS, only clozapine and quetiapine (**3**) are devoid of EPS across the full dose range<sup>11</sup> and atypicals are still prone to other side effects such as weight gain, hyperglycaemia and dyslipidemia. Indeed, the different side effects of atypicals may be equally concerning compared to the motor-related effects of typical antipsychotics. Overall, the side effect profile has a detrimental impact on patient compliance which is still a major challenge in the treatment of schizophrenia.<sup>13,14</sup> Improvement in this regard would therefore have multiple benefits for patient well being and tackle the unmet medical need for antipsychotics with reduced side effect liabilities.

The multireceptor hypothesis, in particular the ratio of interaction between dopamine D<sub>2</sub> and serotonin 5-HT<sub>2</sub> receptors, is often used for rationalising the atypicality of antipsychotics and their incidence of EPS. However, all major atypical antipsychotics fully occupy the serotonin 5-HT<sub>2</sub> receptors at their clinically relevant

\* Corresponding authors. Tel.: +34 925 24 5782 (G.T.), +32 14 60 6016 (X.L.).

E-mail addresses: [gtresade@its.jnj.com](mailto:gtresade@its.jnj.com) (G. Tresadern), [xlangoi@its.jnj.com](mailto:xlangoi@its.jnj.com) (X. Langlois).

dosage but still differ in their propensity to induce motor related side-effects. In addition, typical and atypical antipsychotics give rise to motor side effects at similar levels of occupancy of the D<sub>2</sub> receptor, suggesting the role of interaction with other receptors is not implicated. Alternatively, it has been proposed that typical and atypical antipsychotics can be distinguished by the rates at which they dissociate from dopamine D<sub>2</sub> receptors.<sup>15</sup> Both clozapine and quetiapine have the fastest rate of dissociation from dopamine D<sub>2</sub> receptors whereas antipsychotics associated with a higher prevalence of EPS such as haloperidol are the slowest dissociating dopamine D<sub>2</sub> receptor antagonists. Furthermore, endogenous concentrations of dopamine change by a factor of ten or more in response to certain tasks or challenges.<sup>16–18</sup> The time scale for these changes is dependent on the invoked physiological response but in the fastest cases it occurs in milliseconds.<sup>19</sup> Dopamine binds with high affinity to dopamine receptors and as such the dopamine system functions via fast and small changes in the neurotransmitter concentration. For normal physiological functioning, dopamine receptors of schizophrenic patients should respond to these changes and the antipsychotic ought to dissociate rapidly from D<sub>2</sub> receptors when required.

Within the wider drug discovery context kinetic considerations are increasingly seen as important for the development of new compounds.<sup>20</sup> The affinity of a compound for a receptor, expressed as the dissociation constant, is the ratio of the on and off rates,  $K_d = k_{on}/k_{off}$ .<sup>21</sup> In order to elicit the desired therapeutic effect some biological targets require a longer residence time and slow off rate such as the tyrosine kinase inhibitor Lapatinib.<sup>22</sup> In the case of antagonism of D<sub>2</sub> receptors a fast off rate is a more attractive kinetic profile. For a series of nine D<sub>2</sub> antagonists with three orders of magnitude difference in  $K_d$  their  $k_{on}$  remained essentially constant.<sup>23</sup> The differences in affinity were therefore attributed to  $k_{off}$ , effectively lower affinity dopamine D<sub>2</sub> antagonists were faster dissociating. Up to now this is the only explanation of what can impact and modify the rate of dissociation. The field of study is dominated by analyses of known antipsychotics and in that sense can be considered as a retrospective validation of the hypothesis. Nevertheless, research around a new class of compounds reported as dopamine stabilisers suggests these compounds also display fast dissociating properties and low EPS liabilities.<sup>24–26</sup> One compound from the series, NS30678, was shown to be equipotent with haloperidol and raclopride, 7.0 nM, yet still fast dissociating. This unexpected result suggests that fast dissociation is not simply due to low affinity at the D<sub>2</sub> receptor. It was argued the agonist like structural motif of this class of compounds could be responsible. Here we examine in more detail the properties which affect fast dissociation from D<sub>2</sub> receptors using a large in-house dataset of D<sub>2</sub> antagonists.

As part of our on-going efforts in discovery research to find new treatments for schizophrenia, we have been investigating fast dissociating selective D<sub>2</sub> antagonists. As evidenced by recent patent activity<sup>27</sup> work in our laboratories has focussed on the exemplification of multiple chemical series of novel fast dissociating D<sub>2</sub> antagonists. Biological assays based on [<sup>3</sup>H]spiperone binding displacement have been used to classify the degree and speed of dissociation from the D<sub>2</sub> receptor. As well as the reported novel compounds which were the subject of lead optimisation, many existing compounds from our internal collection were analysed in the same assays. A screen was performed to identify fast dissociating D<sub>2</sub> antagonists as starting points for medicinal chemistry optimisation. As such, an internal database was assembled of over 1800 compounds with considerable chemical diversity and consistently determined binding pIC<sub>50</sub> and fast dissociation data. Here we present a statistical analysis of that dataset and highlight the molecular properties important for distinguishing fast and slow dissociating compounds from the D<sub>2</sub> receptor. It is shown that

despite the inverse correlation with pIC<sub>50</sub>, the rate of dissociation can vary greatly within a small range of pIC<sub>50</sub>. Molecular properties relating to polarity and lipophilicity such as the number of hydrogen bond acceptors, MW and log *P* are important.

## 2. Experimental section

### 2.1. Biological experimental data

Compounds were first screened for their D<sub>2</sub> affinity in a binding assay using [<sup>3</sup>H]spiperone and human D<sub>2</sub>L receptor cell membranes. Frozen membranes of human D<sub>2</sub>L receptor-transfected CHO cells were thawed, briefly homogenised using an Ultra-Turrax T25 homogeniser and diluted in Tris–HCl assay buffer containing NaCl, CaCl<sub>2</sub>, MgCl<sub>2</sub>, KCl (50, 120, 2, 1, and 5 mM, respectively, adjusted to pH 7.7 with HCl) to an appropriate protein concentration optimised for specific and non-specific binding. Radioligand [<sup>3</sup>H]spiperone (NEN, specific activity ~70 Ci/mmol) was diluted in assay buffer at a concentration of 2 nmol/l. Prepared radioligand (50 µl) along with 50 µl of either the 10% DMSO control, Butaclamol, (10<sup>−6</sup> mol/l final concentration), or the compound of interest, was then incubated (30 min, 37 °C) with 400 µl of the prepared membrane solution. Membrane-bound activity was filtered through a Packard Filtermate harvester onto GF/B Unifilterplates and washed with ice-cold Tris–HCl buffer (50 mM; pH 7.7; 6 × 0.5 ml). Filters were allowed to dry before adding scintillation fluid and counting in a Topcount scintillation counter. Percentage specific bound and competition binding curves were calculated using S-Plus software (Insightful).

Subsequently, compounds were tested in an indirect assay adapted from a previously published approach<sup>28</sup> to evaluate their rate of dissociation. Compounds at a concentration of between 4 and 8 times their IC<sub>50</sub> were first incubated for 1 h with human D<sub>2</sub>L receptor cell membranes in a volume of 2 ml at 25 °C, then filtered over a glass fibre filter under suction using a 40 well multivisor. Immediately after, the vacuum was released and 0.4 ml of pre-warmed buffer (25 °C) containing 1 nM [<sup>3</sup>H]spiperone was added on the filter for 5 min. The incubation was stopped by initiating the vacuum and immediate rinsing with 2 × 5 ml of ice-cold buffer. The filter-bound radioactivity was measured in a liquid scintillation spectrometer. The principle of the assay is based on the assumption that the faster a compound dissociates from the D<sub>2</sub> receptor, the faster [<sup>3</sup>H]spiperone binds to the D<sub>2</sub> receptor. When D<sub>2</sub> receptors are incubated with clozapine at the concentration of 1850 nM (4 × IC<sub>50</sub>), [<sup>3</sup>H]spiperone binding is equivalent to 60–70% of its total binding capacity (measured in the absence of other compounds) after 5 min incubation on filter. For our internal discovery efforts to identify fast dissociating compounds, clozapine was included as a reference in each filtration run. Tested compounds were considered as fast dissociating D<sub>2</sub> antagonists if they were dissociating as fast as or faster than clozapine, see definition of slow and fast dissociation described later.

### 2.2. Molecular descriptors

Descriptors were calculated with MOE (Molecular Operating Environment) and ACD (Advanced Chemistry Development). For descriptors calculated in MOE<sup>29</sup> firstly the molecules were imported in 2D and the protonation state was assigned using the wash function. Visual inspection was performed to check that all molecules were protonated as expected for D<sub>2</sub> antagonists. In particular this meant correcting molecules which had been protonated twice. Hydrogens were added and charges calculated using the MMFF94x force field, 184 2D descriptors were calculated using the MOEdb compute descriptors function. Descriptors were successfully calculated for all 1863 compounds.

Additional descriptors were calculated with the ACD labs software.<sup>30</sup> Molecules were imported in a 2D unionised format. ACD failed to calculate descriptors for a small number of compounds; these compounds were removed which reduced the dataset to 1825 compounds. Finally, those with missing descriptor values or extreme outlier values in any of the descriptors were removed leaving a total set of 1816 compounds. This entire dataset was used as input for the descriptor selection process.

### 2.3. Statistical analyses

A combination of univariate and multivariate approaches were used. For the univariate analysis the descriptors were inspected via their Pearson correlation coefficients to fast dissociation. These were calculated using the in-house program ABCD.<sup>31</sup> In addition univariate ANOVA (analysis of variance) analysis was performed to demonstrate the difference in average descriptor values for fast and slow dissociating compounds. All ANOVA work was done using the STATISTICA 9.0 program.<sup>32</sup> Different multivariate statistical techniques were used which included principal component analysis (PCA) and partial least squares (PLS) regression.

The combination of 1816 molecules and a large number of potentially correlated descriptors yielded a matrix. PCA is well suited to analysis of such a dataset as it reduces the matrix and its correlated descriptors into a smaller matrix of uncorrelated, orthogonal variables called principal components. The process yields three new matrices; the loadings matrix **P**, the scores **T** and the residuals **E**. The loadings describe the information of the original descriptors via the principal components. The scores contain information about the molecules, described in terms of their projection into the principal components. The residual matrix, **E**, contains the information not described by the product of loadings and scores. The descriptors which influence each PC and therefore have the biggest impact on differentiating the input compounds can be readily identified.

PLS regression was employed in order to understand the role of the descriptors in explaining fast dissociation. In more detail, the dataset was split into two classes, fast and slow dissociating compounds, and PLS discriminant analysis (PLS-DA) was performed. For our internal discovery efforts we considered a fast dissociating compound to be one which dissociates faster than clozapine (60–70%). Hence for this analysis, fast dissociation was defined for any compound with  $\geq 70\%$  dissociation of [<sup>3</sup>H]spiperone binding, and slow dissociation was  $\leq 30\%$ . This approach reduced the dataset to 939 compounds and the two classes were of similar size, 498 were fast and 441 slow dissociating. Setting these limits and performing the analysis in terms of the two classes was also suitable given the standard deviation in dissociation rate. Replicate experiments performed on the same compounds revealed a standard deviation of 7%. Assuming a normal distribution there is 99% confidence that compounds lie within approximately 2.6 standard deviations of their measured values. Omitting a 40% range between the slow and fast classes means there is little chance that a compound close to the boundary of either group is misclassified. All data for multivariate analysis were normalised by mean centering and scaled to unit variance. Descriptors containing no variance from the mean were removed. The SIMCA P+12 software was used throughout.<sup>33</sup> The cross validated  $q^2$  was calculated in SIMCA leaving out a 7th of the data and predicting their dissociation class and comparing to their actual values. To confirm that the PLS models could not have occurred by chance, Y-randomisation was performed on the input dataset within SIMCA. A total of 999 training sets were generated by scrambling the fast dissociation class for each compound whilst keeping the descriptors intact. In all cases,  $r^2$  for the random models was less than 0.2 and  $q^2$  never exceeded

0.1, confirming the models constructed herein were vastly superior to random and unlikely to be spurious.

## 3. Results

### 3.1. Descriptor selection

The intention of this work was to use statistical analysis to understand the properties affecting fast dissociation from the D<sub>2</sub> receptor rather than deriving the optimal model to be used for virtual screening. There are thousands of available descriptors and if combined correctly with appropriate modelling workflows they can be used with excellent results.<sup>34</sup> Nevertheless, given our interest in interpretability we defined a set of intuitive molecular descriptors that were well suited to this dataset. It has been shown<sup>35,36</sup> and is also our experience that for global analyses covering multiple chemical series a sufficient amount of chemical diversity is captured with few principal components influenced by descriptors of size (MW), polarity or lipophilicity (PSA and log *P*), and charge (p*K*<sub>a</sub>). Indeed, we have a preferred list of comprehensible descriptors which form a starting point for most attempts at statistical design, Table 1. Descriptors such as MW, log *D*, log *P*, p*K*<sub>a</sub> and H-bond acceptor and donor counts all form a part of this set and were included in this work because of their value for capturing molecular diversity and their interpretability. For the calculation of properties relating to ionisation such as p*K*<sub>a</sub> and log *D*, the ACD software was used. This tool showed good performance in a recently published analysis.<sup>37</sup> To identify further dataset specific descriptors the MOE software was used. The available set of 184 2D descriptors in MOE includes atom and bond counts, connectivity indices, subdivided surface area descriptors, partial charge descriptors, calculated physicochemical properties, etc. We set out to identify if any of these additional descriptors would be of value for this dataset.

**Table 1**  
Descriptors used throughout this study

Descriptor ID	Details
log <i>P</i>	log <i>P</i> calculated with ACD
log <i>D</i> <sub>2</sub>	log <i>D</i> at pH 2, calculated with ACD
log <i>D</i> <sub>5.5</sub>	log <i>D</i> at pH 5.5, calculated with ACD
log <i>D</i> <sub>6.5</sub>	log <i>D</i> at pH 6.5, calculated with ACD
log <i>D</i> <sub>7.4</sub>	log <i>D</i> at pH 7.4, calculated with ACD
log <i>D</i> <sub>10</sub>	log <i>D</i> at pH 10, calculated with ACD
p <i>K</i> <sub>a</sub> -MB	The most basic p <i>K</i> <sub>a</sub> , calculated with ACD
p <i>K</i> <sub>a</sub> -MA <sup>a</sup>	The most acidic p <i>K</i> <sub>a</sub> , calculated with ACD
mr	Molecular refractivity calculated with ACD
MW	Molecular weight
PSA	Polar surface area
nRB	Number of rotatable bonds
HBA	Number of H-bond acceptors
HBD	Number of H-bond donors
Rings	Number of rings
vdw_vol	Volume calculated with a 2D method
Descriptors selected for their applicability to this dataset	
a_hyd	Number of hydrophobic atoms
log <i>S</i>	Log of the intrinsic solubility (mg/ml)
Chiral	Number of chiral centres
BCUT_s log <i>P</i> <sub>2</sub>	BCUT using atomic contribution to log <i>P</i>
PEOE_RPC+	Relative positive partial charge, largest charge divided by sum of charges
Fcharge	Total charge on the molecule
a_nF	Number of fluorine atoms
a_nN	Number of Nitrogen atoms
b_double	Number of double bonds

<sup>a</sup> Calculated for the dataset but removed from the multivariate modelling as there were too many missing values, 73% of compounds did not have an acidic p*K*<sub>a</sub>.



Extra descriptors were of value if they captured elements of either the biological response (extent of dissociation) or the diversity of the molecular space. To tackle the first issue a univariate correlation analysis of the MOE 2D descriptors was performed. The approach revealed 41 descriptors with a Pearson correlation coefficient  $>0.25$  or  $<-0.25$  to the percent of dissociation, see Table S1 in Supplementary data. A coefficient greater than 0.25 indicated positive correlation to fast dissociation and a coefficient less than  $-0.25$  negative correlation. It was apparent that many of these descriptors were in turn highly correlated with each other and therefore redundant. For instance, the number of atoms (a\_count) and the number of heavy atoms (a\_heavy) have a correlation coefficient of 0.95 ( $r^2 = 0.90$ ). Principal component analysis (PCA) offers an ideal way for reducing the descriptors to fewer uncorrelated principal components. This approach was applied to the matrix of compounds and 41 descriptors. Five descriptors were chosen that were influential in the first four principal components. The first four PCs described 90% of the variation in the 41 descriptors. The five descriptors were selected from different areas of the loadings plot; more details are given in the Supplementary data. The chosen descriptors were the number of hydrophobic atoms (a\_hyd), log of the aqueous solubility (log S), the number of chiral atoms (chiral), a BCUT descriptor based on atomic contribution to lipophilicity (BCUT\_s log P\_2), and the relative positive partial charge (PEOE\_RPC+).

To select descriptors which captured the diversity of the compounds a second PCA analysis was performed. However, in this case the entire set of 2D MOE descriptors for all compounds was analysed. Further details can be found in the Supplementary data. The analysis revealed that four additional descriptors had a strong influence on the PCs and would therefore be useful for capturing the variation in the total descriptor space. The four descriptors included were: the total charge on the molecule (FCharge), the number of Fluorine atoms (a\_nF), the number of nitrogen atoms (a\_nN), and the number of double bonds (b\_double). Therefore nine additional descriptors suitable for this dataset were combined with those frequently used for multivariate analysis providing a total set of 25 descriptors used throughout the rest of this study, Table 1.

### 3.2. Composition of the entire dataset

The complete dataset contained over 1800 compounds which were all evaluated in two biological assays to measure their affinity for the D<sub>2</sub> receptor and their degree of dissociation. The binding pIC<sub>50</sub> was measured by displacement of [<sup>3</sup>H]spiperone. The dissociation was measured via an indirect approach also making use of tritiated spiperone. The details are given in the experimental section but the principle of the assay was the faster a compound dissociates from the D<sub>2</sub> receptor after a 1 h incubation period the faster [<sup>3</sup>H]spiperone binds to the receptor. Figure 1 shows a scatter plot of the extent of dissociation and pIC<sub>50</sub> for each compound. The pIC<sub>50</sub> covers a four log unit range from 5.0 to 9.34 (10,000–0.45 nM), and the dissociation measurement varies from 5% (almost no dissociation) to 100% (full dissociation) and above (116% due to experimental variability). Compounds with pIC<sub>50</sub> below the measured concentration limit, that is, pIC<sub>50</sub> <5, were not included in this dataset. The distribution of pIC<sub>50</sub> was Gaussian shaped and centred on 7.1 (both the mean and median equal 7.1). As described in the introduction the two properties should be inversely correlated and indeed that can be seen in Figure 1, the Pearson correlation coefficient was  $-0.52$ . The compounds in the dataset contained many chemical scaffolds and motifs familiar to researchers in D<sub>2</sub> receptor antagonism. Tricyclic compounds such as clozapine, benzamides similar to amisulpride and butyrophenone derivatives such as haloperidol were all present. In addition there were examples of series such as aminopyridines,

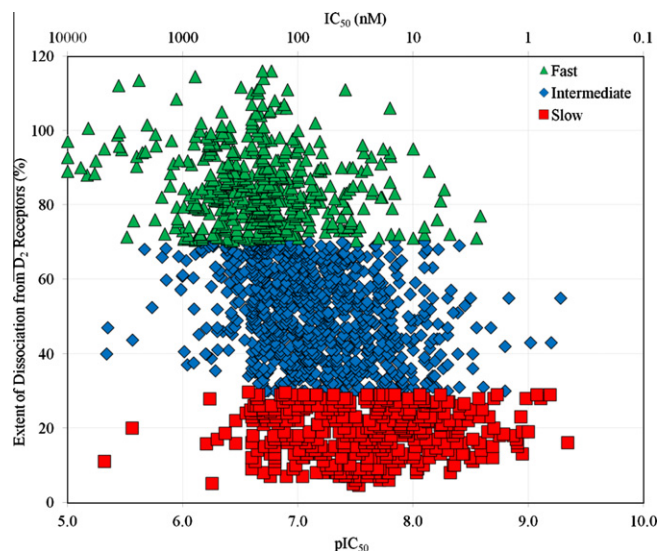


**Figure 1.** Scatter plot showing the extent of dissociation versus binding affinity (pIC<sub>50</sub>) at the D<sub>2</sub> receptors for each compound in the dataset. Extent of dissociation represents the speed which each compound dissociates from the D<sub>2</sub> receptors after addition of [<sup>3</sup>H]spiperone, see the experimental and composition of the entire dataset sections for more details.

aminothia(di)azoles and pyridazines, which have been pursued as part of our recent work searching for novel and selective fast dissociating D<sub>2</sub> receptor antagonists. The molecules in Figure 1 are coloured by the classification of the rate of dissociation from the D<sub>2</sub> receptor which is explained in the following sections.

To shed further light on this proprietary dataset common ring substructures were extracted. Pipeline pilot was used to identify the most frequently occurring ring and Murcko fragment assemblies<sup>38</sup> and the results are shown in Figure 2. Not surprisingly for a series of D<sub>2</sub> antagonists, aromatic and protonatable amine ring substructures such as phenyl, piperidine and piperazine were numerous in this dataset. The tetracyclic tetrahydrofurans which have been previously explored in our laboratories<sup>39</sup> were frequent within the dataset, 222 examples. Many of the common bicyclic ring systems such as benzisoxazole, bezimidazolone and benzisothiazole are recognisable from antipsychotics such as risperidone (4), iloperidone, droperidol and ziprasidone. Also in Figure 2, histograms of simple descriptors log P, MW and polar surface area (PSA) are compared. All plots show unimodal behaviour. The majority of molecules had a MW <500 although the distribution tails to relatively high MW due to a small number of larger compounds in this dataset. The compounds were quite highly lipophilic with a mean log P of 4.5. Since many of these compounds were targeted for CNS application their polar surface area is relatively low with a mean average of 45.

Known D<sub>2</sub> antagonist reference compounds were present in this dataset. The biological assay for determining the extent of dissociation from the D<sub>2</sub> receptor was validated by comparing the association of [<sup>3</sup>H]spiperone in presence of a series of reference compounds. The structures of haloperidol (1), clozapine (2), quetiapine (3), risperidone (4) and flupentixol (5) are all given in Figure 3. Each compound was incubated with D<sub>2</sub> receptors for 60 min at a concentration equal to 4 times their IC<sub>50</sub>. After filtration, [<sup>3</sup>H]spiperone was added on the compound-membrane mixture retained on filters and the time course of [<sup>3</sup>H]spiperone binding in presence of the different compounds is shown in Figure 4. As mentioned previously, the assay assumes that the faster a compound dissociates from the D<sub>2</sub> receptors the faster spiperone will bind. Within the fast dissociation hypothesis,

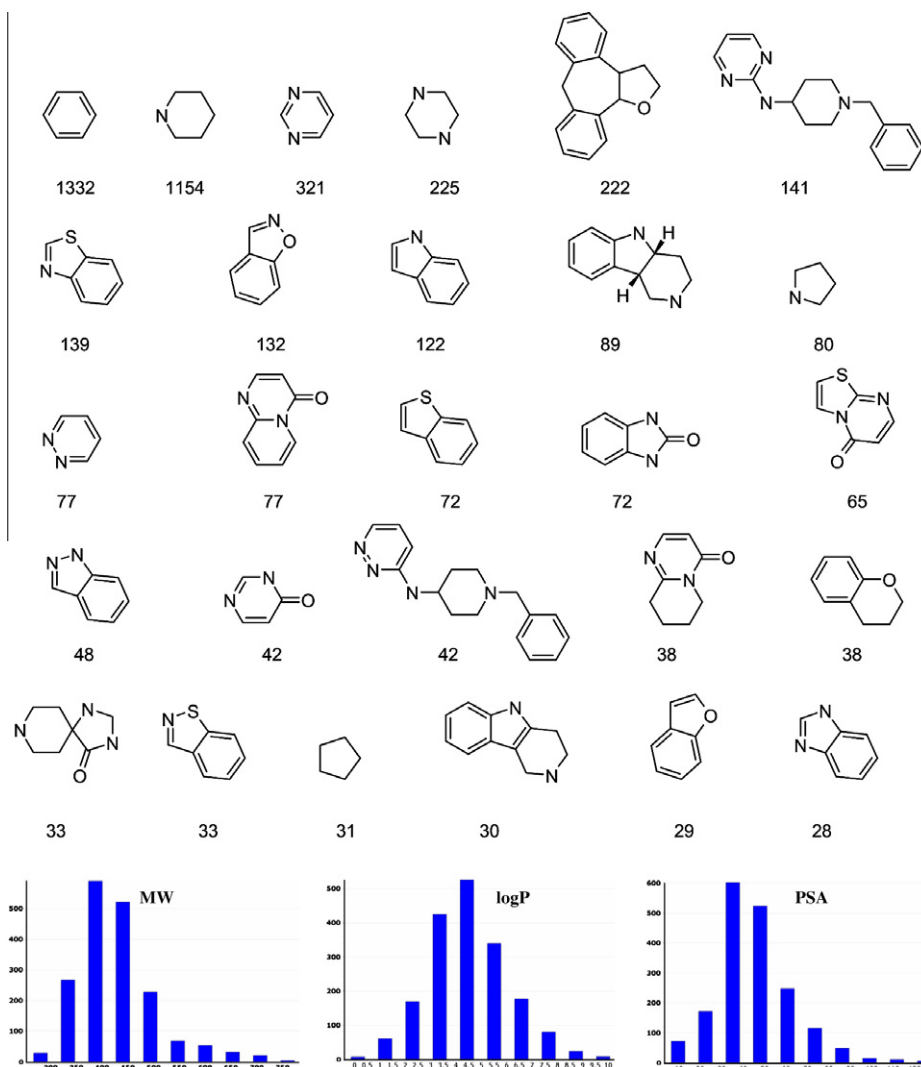


**Figure 2.** Details of the dataset. The most common ring and Murcko substructures present within the dataset, the number denotes the frequency of occurrence. Distributions of MW, log *P* and polar surface area (PSA).

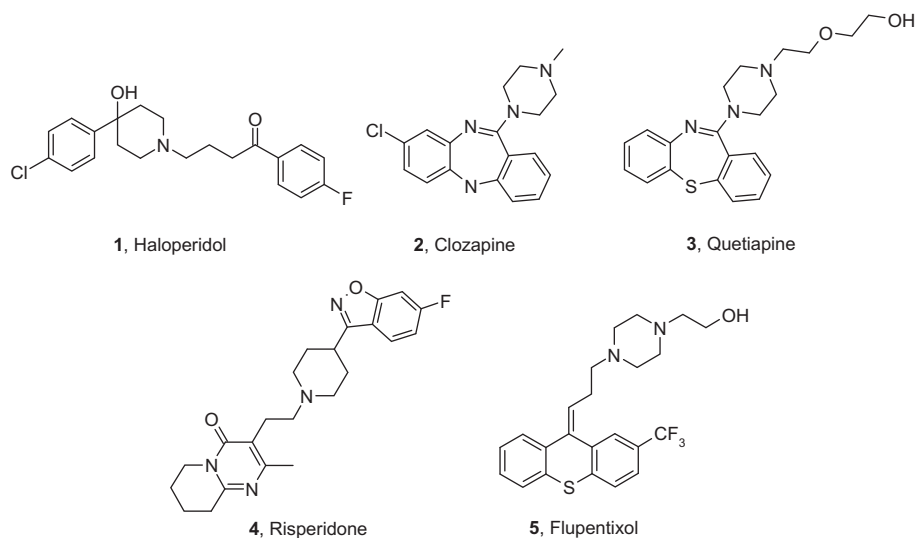


**Figure 3.** D<sub>2</sub> antagonist reference compounds.

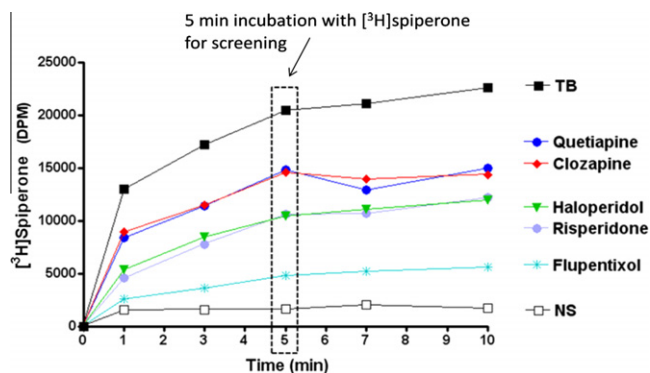


**Figure 4.** Evaluation of the dissociation speed of reference antipsychotics by measuring the binding association of [ $^3\text{H}$ ]spiperone in absence (TB) or presence of drugs (clozapine, quetiapine, haloperidol, risperidone, flupentixol incubated at a concentration equal to 4 times their  $\text{IC}_{50}$ ). The dashed line box indicates how drugs differentiate from each other after a 5-min incubation with [ $^3\text{H}$ ]spiperone, which is the time point chosen for the screening of our compound database.

clozapine is held as the standard and benchmark for a fast dissociating compound. It can be seen that at the 5-min time point clozapine was amongst the fastest dissociating of the compounds in Figure 4. Therefore, despite the relatively simple indirect method for assessing the rate of dissociation this approach was able to discriminate clozapine as the fastest of the reference antipsychotics. Also, our data shows that flupentixol is a particularly slow dissociating compound, as it was described in the original method (Ref. 28). Accordingly, a 5-min incubation with [ $^3\text{H}$ ]spiperone was chosen as the most appropriate time point (practical enough and being able to discriminate fast from slow dissociating antagonist) for the screening of our database. In addition, lead compounds from our internal discovery efforts which were identified as fast dissociating  $\text{D}_2$  receptor antagonists in this assay were confirmed subsequently upon more detailed evaluation.

As mentioned in the experimental section, the dataset was partitioned into two classes to qualitatively describe the dissociation properties. Compounds with >70% fast dissociation were classified as fast, those with <30% as slow. The intermediate compounds, with dissociation between 30% and 70% were discarded from the subsequent PLS-DA. Overall this dataset comprised many different chemical series and it should be expected that the significant chemical diversity would prohibit the identification of strong QSAR relationships.

### 3.3. Univariate statistical analysis

After classifying compounds as either fast or slow dissociating a relatively straightforward one-way ANOVA analysis was performed. This approach compares the mean of each descriptor within the fast and slow dissociating classes. Any statistically relevant differences can be rapidly gleaned. The methodology provides significant advantages in terms of interpretability compared to the more sophisticated multivariate approaches presented later. The resultant plots for all descriptors are given in the [Supplementary data, Figure S3](#). Selected examples with statistically significant differences between fast and slow classes are shown in Figure 5. As described above some of the molecular descriptors were selected based on their Pearson correlation coefficient with the extent of dissociation. Therefore it should come as no surprise that they are appropriate for differentiating between the fast and slow dissociating classes. Lipophilicity was clearly important; all  $\log D$  descriptors,  $\log P$  and the number of hydrophobic atoms were lower for fast dissociating compounds compared to slow. Likewise size plays a role; MW, molecular volume, the number of rings and

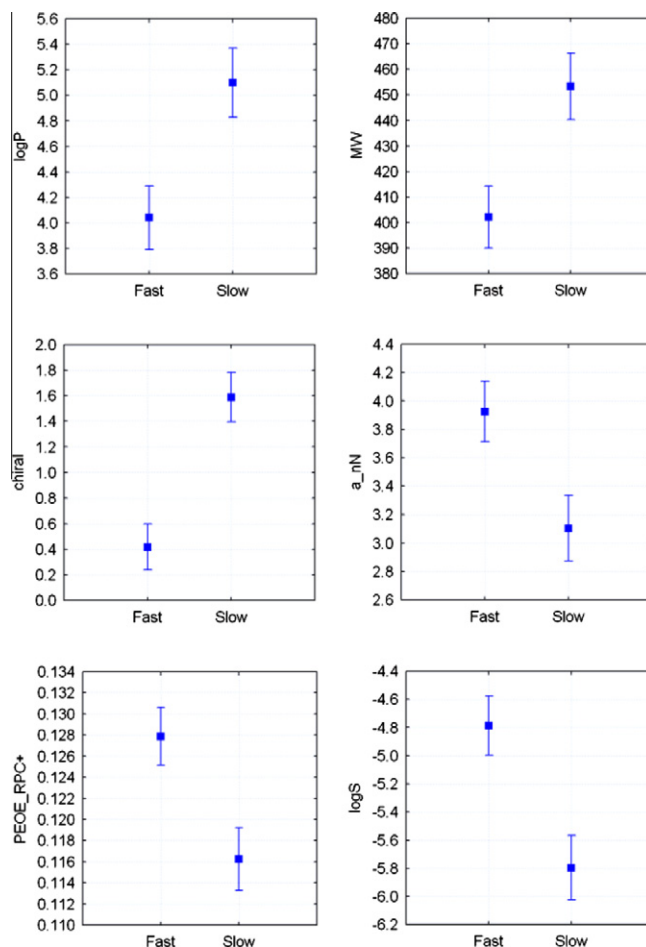


**Figure 5.** Selected descriptors ( $\log P$ , MW, chiral,  $a_{\text{nN}}$ , PEOE\_RPC+ and  $\log S$ ) which showed significant difference between fast and slow dissociating  $\text{D}_2$  receptor antagonists. The plots were derived via one-way ANOVA analysis and show the mean of each descriptor for the corresponding fast and slow classes. The whiskers/bars indicate the 99.9% confidence interval.

double bonds were all lower for the fast class. The number of chiral centres was also lower for fast dissociating compounds. Fast dissociating compounds had more nitrogen atoms ( $a_{\text{nN}}$ ), higher positive partial charge (PEOE\_RPC+) and a higher predicted solubility ( $\log S$ ). These results provide the first indications of the differences between fast and slow dissociating compounds. The former are characterised as more polar, less lipophilic and with lower MW.

### 3.4. Multivariate statistical analysis

Multivariate PLS-DA was performed on the fast and slow classified compounds to understand in more detail the important descriptors. To begin with all fast or slow dissociating compounds across the whole range of  $\text{pIC}_{50}$  were studied. After setting aside 10% of the dataset to be used as a subsequent test set, the statistical model was built from the remaining 827 compounds with measured  $\text{pIC}_{50}$  and dissociation rate. The fast dissociating class contained 444 compounds and the slow class 383. The resulting PLS model had a modest  $r^2$  of 0.53 whilst the cross validated  $q^2$  was similar, 0.52, which suggests that the model was not over-fitted. The model correctly classified 74% of the compounds into their fast or slow class. This was respectable performance considering the size and diversity of the dataset being studied. The model was then assessed with the test set of 92 compounds which had not been used during model construction. This is often seen as a

better test of the validity of such statistical models. The test set was selected randomly and contained 48 compounds from the fast class and 44 from the slow class. Performance was almost identical to the cross-validation performed within the model, 75% of the external compounds were correctly classified. The distance to model is the distance of a compound to the hyperplane of descriptor space captured in the PLS model. In essence it provides a metric of how close compounds are to the model and helps understand the risk of extrapolation versus interpolation when applying the model. A model would be expected to perform well for compounds with a low distance to model metric.<sup>40</sup> In this case 70 of the compounds in the test set were within a distance to model of 1 and the overall mean distance to model was 0.9. The mean distance to model for compounds in the training set was also 0.9. The overall good performance of the model with both internal cross-validation and the subsequent test set confirm the model is robust and not over-fitted to the compounds used during its construction.

Figure 6 shows the scores and loadings plot for the model built from slow and fast dissociating compounds across the entire range of  $pIC_{50}$ . The scores are the new orthogonal variables generated by the model which summarise the descriptors for the molecules. The two components in the plot describe approximately 50% of the overall variance in the descriptors. The tolerance ellipse is based on Hotelling's  $T^2$ , compounds outside the ellipse are outliers. It can be seen that there is small group of outliers in the bottom right quadrant but the majority of compounds are located within the ellipse. In addition there is relatively even distribution across the descriptor space suggesting there are no structural clusters dominating the model. The model separates the fast and slow compounds well, but with some overlap in the centre of the plot. The loadings plot demonstrates the relationship between the descriptors and the degree of fast dissociation. The fast and slow dissociation responses are identified as green triangle and red square, respectively. As expected they are opposite to each other with respect to the origin of the plot. The descriptors near the biological response, either fast or slow dissociation, are positively correlated to them. In this case fast dissociation correlates positively with increasing the number of nitrogen atoms ( $a_{nN}$ ) and the number of rotatable bonds ( $nRB$ ). Slow dissociation correlates with increasing the BCUT  $s \log P$  descriptor ( $BCUT\_s \log P_2$ ), the number of double bonds ( $b\_double$ ), the number of rings ( $rings$ ) and the number of chiral centres ( $chiral$ ). These descriptors were in agreement with those revealed by the univariate ANOVA analysis.

Whilst this model sheds further light on the properties affecting fast dissociation, it is known from Figure 1 that the rate of dissociation is inversely correlated with the binding affinity ( $r^2$  of 0.27). This is intuitive as weaker binding compounds would be expected to be faster dissociating. Indeed, we re-built a multivariate PLS discriminant model as just described but this time included the  $pIC_{50}$  for each compound as a descriptor. Not surprisingly the resultant model was statistically better, with an  $r^2$  of 0.64 and cross validated  $q^2$  of 0.62. The  $pIC_{50}$  was the most important descriptor in this model. Therefore it is possible that the multivariate model discussed above may be capturing elements which explain the binding affinity and in turn its inverse relationship to the rate of dissociation. This issue was studied in more detail. It can be seen from Figure 1 that within small ranges of  $pIC_{50}$  there is still a large variation in the degree of dissociation. This suggests that despite having similar binding affinity some compounds are fast whilst others are slow dissociating. Multivariate statistical analysis was applied to compounds within small ranges of  $pIC_{50}$  thereby nullifying the inverse correlative effects of binding affinity. Our approach can be considered analogous to that used recently to study the effects of solid-state limited solubility where it was of interest to understand what affects the solubility when compound lipophilicity is assumed constant.<sup>41</sup>

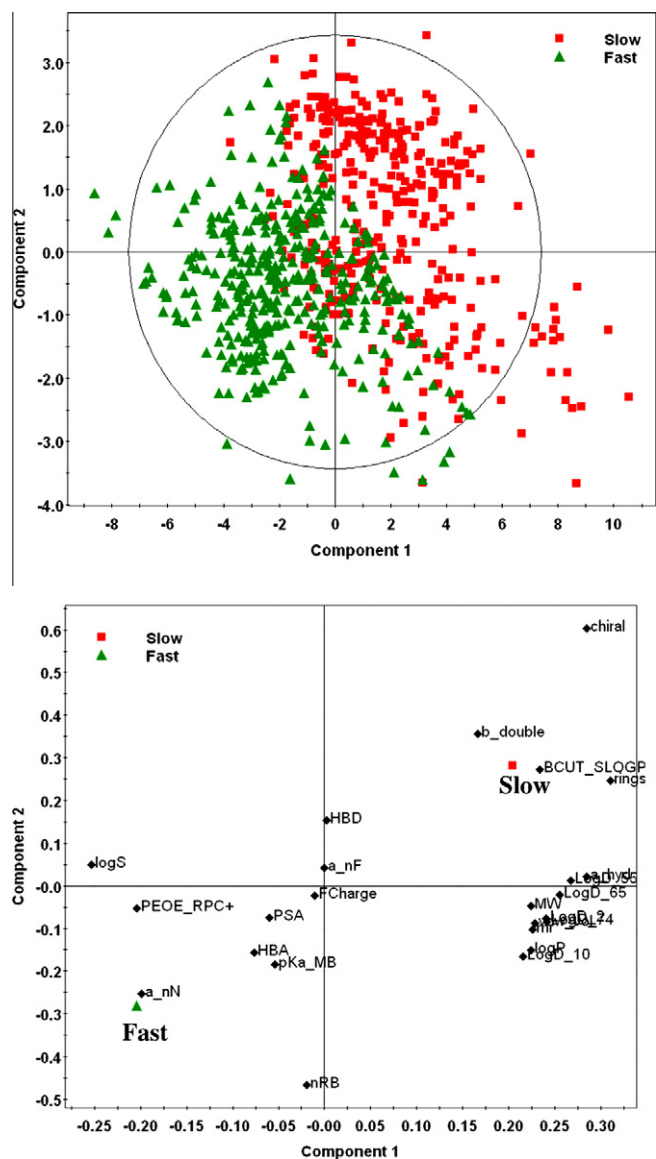


**Figure 6.** The scores plot (top) and loadings plot (bottom) from the multivariate PLS discriminant model built from all fast and slow dissociating compounds across the  $pIC_{50}$  range. The scores plot shows the distribution of the compounds in the new component space, fast dissociating compounds are labelled as green triangles whereas slow dissociating compounds are red squares. In the loadings plot the location of the fast (green triangle) and slow (red square) response is shown with respect to the molecular descriptors.

The dataset was partitioned by defining four ranges of  $pIC_{50}$ , from 6.5 to 6.75, 6.75 to 7.0, 7.0 to 7.25 and 7.25 to 7.5, see Figure 7. Importantly there was no longer any inverse correlation between binding affinity and rate of dissociation within these  $pIC_{50}$  ranges, the  $r^2$  being 0.02 in the largest case, confirming that the rate of dissociation was independent of binding affinity. Compounds defined previously as either fast or slow dissociating within these bins of  $pIC_{50}$  were in turn subjected to multivariate PLS-DA. Four separate models were built as shown in Table 2. Each bin of binding affinity still contained an acceptable number of compounds for this type of modelling, from 79 in the least case to 137 in the most. The PLS models were built with the same 25 descriptors used throughout this study. All descriptors were retained in each model to facilitate the subsequent side by side comparison and understand their role. The corresponding  $r^2$  and  $q^2$  for each model were better than for the model described above built across



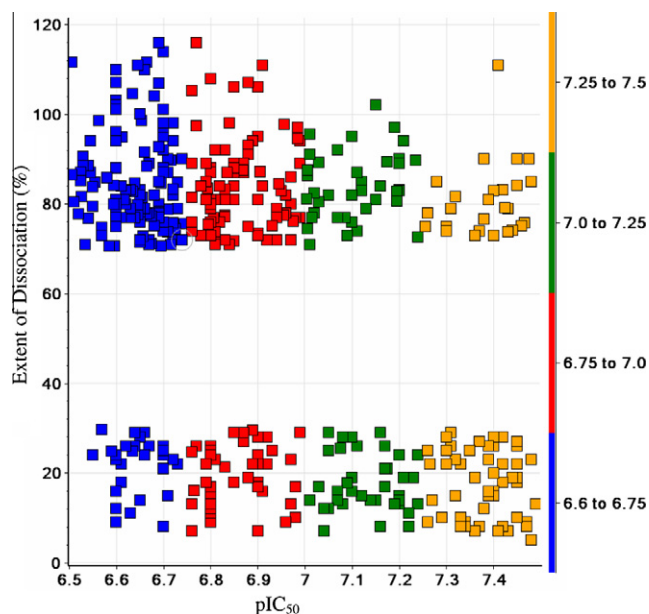


**Figure 7.** Graphical representation of how the dataset was partitioned into ranges of  $pIC_{50}$  which were subsequently subjected to multivariate PLS and two-way ANOVA analysis.

the entire range of  $pIC_{50}$ . External validation of each model was performed by testing its performance on the compounds in the other three ranges of binding affinity. The percentage of compounds correctly classified from the external validation is often very close to that seen for the compounds within the model. For instance, in the case of the model built with compounds in  $pIC_{50}$  range of 7.25–7.5, the model correctly classified 77% of the compounds used during its construction. Subsequently, in the external validation it correctly classified between 61% and 73% of compounds from the other ranges of  $pIC_{50}$ . This represents little deterioration in performance and suggests that overall the model is not over-fitted. The model built from  $pIC_{50}$  range 6.5–6.75 performed worse under external validation and only classified 47% of the compounds from the 7.25 to 7.5  $pIC_{50}$  range. The worse performance may be partly understood by consideration of the distance to model. Table 3 provides the mean distance to model for the compounds in each  $pIC_{50}$  range when applied to the four models. This case was amongst the worst, 45 of the compounds had a distance to model greater than 1 and the mean distance to model was 1.2 whereas it had only been 0.9 for the training set.

The coefficient plots in Figure 8 show how strongly the molecular descriptors in each of the PLS-DA models correlate to the extent of dissociation. The bars represent the 95% confidence interval and the coefficient is significant when the confidence interval does not cross zero. For the model built from compounds across the entire  $pIC_{50}$  range the plot confirms the role of the important descriptors discussed previously and identified via the

**Table 3**

Mean distance to model for compounds in each 0.25 log unit range in  $pIC_{50}$  compared to the PLS-DA models built from compounds within each corresponding range of activity

Model	Mean distance to model for compounds in the specified $pIC_{50}$ range			
	6.5–6.75	6.75–7.0	7.0–7.25	7.25–7.5
$pIC_{50}$ -6.5–6.75	0.9	1.0	1.2	1.2
$pIC_{50}$ -6.75–7.0	0.9	0.9	1.0	1.0
$pIC_{50}$ -7.0–7.25	0.9	0.9	0.9	0.9
$pIC_{50}$ -7.25–7.5	1.2	1.3	1.3	0.9

loadings plot in Figure 6. Increasing the number of nitrogens and rotatable bonds positively correlate with fast dissociation whereas increasing the number of double bonds, chiral centres, rings and BCUT  $s$  log  $P$  descriptor all negatively correlate with fast dissociation. The plot also reveals that hydrogen bond acceptors (HBA), predicted solubility (log  $S$ ), basicity ( $pK_{a-MB}$ ) and partial positive charge (PEOE\_RPC+) all positively correlate with fast dissociation. For the models built over small ranges of  $pIC_{50}$  additional and different descriptors play a role. The plots show that the models contain many insignificant descriptors, so close inspection is required to identify those which are important. Descriptors which positively correlate with fast dissociation in these cases include polar surface area, calculated solubility (log  $S$ ), partial positive charge (PEOE\_RPC+) and log  $D$  at pH 10 (log  $D_{10}$ ) which are all important in two models each. Hydrogen bond donors and acceptors are important in one model each. Interestingly, the number of nitrogens is positively correlated in three models but negatively impacts fast dissociation in one model, suggesting local effects of a particular chemical series dominate in one case. Descriptors which negatively correlate with extent of dissociation include number of hydrophobic atoms ( $a_{hyd}$ ), molecular weight, number of double bonds, number of rings and number of fluorine atoms. The number of hydrophobic atoms is significant in all four models, MW in three models, and the number of double bonds, rings and fluorine atoms in two. Inspection of the details of these smaller models is more challenging as local effects due to particular chemical series become influential, nevertheless, descriptors capturing polarity and lower lipophilicity characterise the fast dissociation compounds.

### 3.5. Two-way ANOVA analysis

The purpose of studying the small ranges of  $pIC_{50}$  was to directly identify the descriptors which influence only the rate of dissociation and do not have an indirect effect on dissociation via the compound affinity. After considering the coefficients plots in Figure 8 it is clear that some descriptors are important within certain  $pIC_{50}$  ranges and not others. In contrast to most traditional QSAR analyses this dataset is highly diverse and there are multiple chemotypes and scaffolds represented even within each  $pIC_{50}$  bin. This complicates the analysis and means that trends are less clearly

**Table 2**

PLS discriminant models to predict fast or slow dissociation from within a small 0.25 log unit range of  $pIC_{50}$

Model	Number of compounds	Number of components	$r^2$	$q^2$	External validation: % of compounds correctly classified from the $pIC_{50}$ range			
					6.5–6.75	6.75–7.0	7.0–7.25	7.25–7.5
$pIC_{50}$ -6.5–6.75	137	4	0.67	0.54	(86%)	74%	60%	47%
$pIC_{50}$ -6.75–7.0	109	2	0.66	0.60	80%	(79%)	63%	56%
$pIC_{50}$ -7.0–7.25	82	2	0.63	0.49	75%	64%	(79%)	72%
$pIC_{50}$ -7.25–7.5	79	3	0.67	0.55	69%	61%	73%	(77%)

External validation of each model was performed by estimating the percent of compounds correctly predicted from the other three datasets not used during model building. For comparison the same measure of classification accuracy is shown in parenthesis for the internal set of compounds used to build each model.



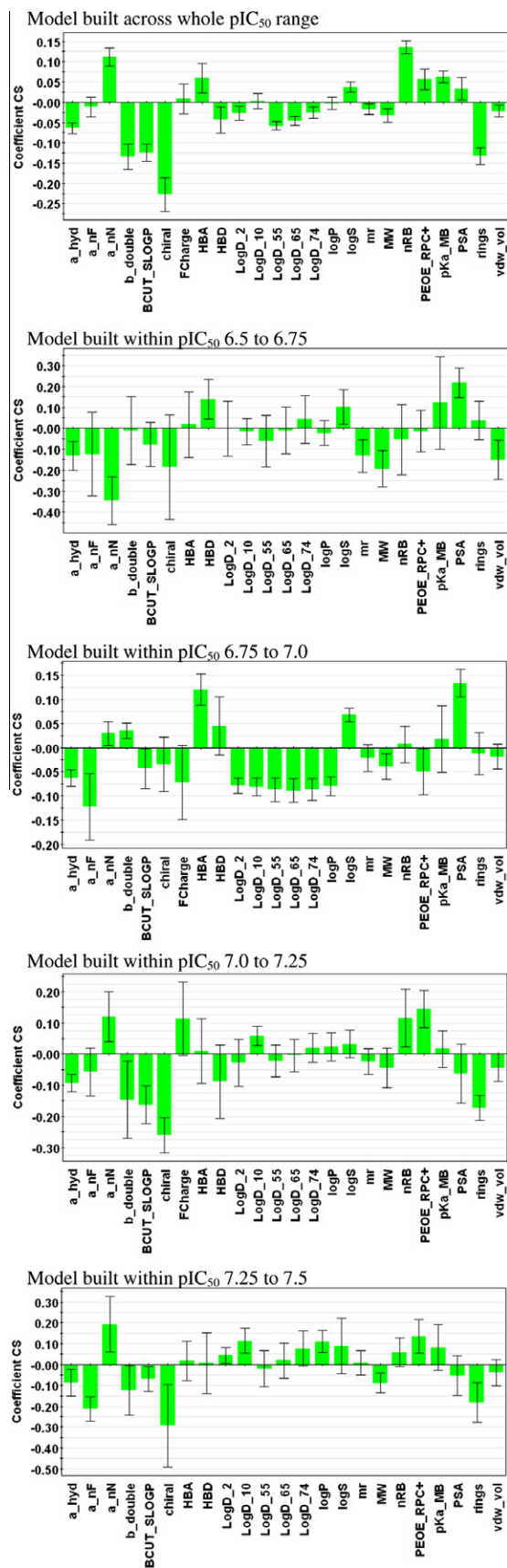


**Figure 8.** Variable coefficients showing the relative correlation of each descriptor to fast dissociation in each of the multivariate PLS discriminant models. Bars indicate 95% confidence interval.

seen. Therefore, to help decipher the molecular properties influencing the dissociation rate independent of affinity, that is, within each bin, we turned to two-way ANOVA analysis. In this approach the mean for each descriptor within fast and slow classes was plotted across the same four  $pIC_{50}$  bins. A selection of interesting descriptors is shown in Figure 9 and the plots for all descriptors are in the Supplementary data, Figure S5. The important lipophilic descriptors revealed in the previous analyses are higher amongst the slow dissociating compounds than the fast ones. This is seen in the  $\log P$  and number of hydrophobic atoms ( $a_{hyd}$ ) although the confidence intervals overlap for the highest affinity bins. Descriptors of molecular size, MW and number of rings, suggest larger molecules have slower dissociation, again with some overlap of confidence intervals for particular  $pIC_{50}$  ranges. The fast dissociating compounds have a higher predicted solubility ( $\log S$ ). Partial positive charge ( $PEOE\_RPC+$ ) and the number of nitrogen atoms ( $a_{nN}$ ) are generally higher for fast dissociating compounds, however, the confidence intervals for each dissociation class overlap for many of the  $pIC_{50}$  bins. The number of chiral centres was a significant descriptor for differentiating fast and slow dissociation at the highest two  $pIC_{50}$  bins, for which many other descriptors did not perform. In summary, we can firmly conclude that descriptors for size and lipophilicity are directly affecting the dissociation of  $D_2$  antagonists from the  $D_2$  receptor independent of compound affinity.

#### 4. Discussion and conclusions

Following the detailed analysis of the multivariate models the picture becomes clear that hydrophobic properties are detrimental for fast dissociation whereas increasing hydrophilic nature measured via descriptors such as number of number of nitrogen atoms, partial positive charge or reducing  $\log P$  seems to have a positive effect on the extent of dissociation. At first thought these conclusions might be readily attributed to the widely understood phenomenon that increasing lipophilicity results in increased binding affinity and as such the results presented here would only be capturing the inverse relationship between  $K_d$  and  $k_{off}$ . There is a chance that such artefacts could have played a role in the model built with all compounds across the full range of  $pIC_{50}$ . However, we have shown that these general conclusions hold true even across narrow ranges of binding affinity where there was no inverse correlation between  $pIC_{50}$  and rate of dissociation.

We can only speculate as to why the hydrophilic/hydrophobic character is important for differentiating fast and slow dissociating molecules despite similar binding affinity. Ligand–protein binding is a complex thermodynamic process involving compensating enthalpic and entropic terms between ligand–protein and solvent.<sup>42,43</sup> The binding affinity can be considered as the free energy difference between bound (protein) and free (solvated) states. Small changes in molecular structure may impact on either or both of these terms. As such the  $k_{on}$  and  $k_{off}$  are influenced by the respective enthalpy and entropy terms for both the ligand–protein and ligand–solvent systems. Hydrogen bonding and electrostatic descriptors likely capture enthalpic components whereas lipophilicity and flexibility descriptors describe the entropic terms associated with for instance the hydrophobic effect. In an indirect way this analysis could be revealing the importance of these thermodynamic properties on fast dissociation from the dopamine  $D_2$  receptor. Binding enthalpy decreases with molecular size and compounds with higher enthalpy are more polar and less lipophilic.<sup>44</sup> It has been shown from thermodynamics experiments that the enthalpy and entropy of ligand binding at the  $D_2$  receptor is discerned by lipophilicity and not by functional effect of the

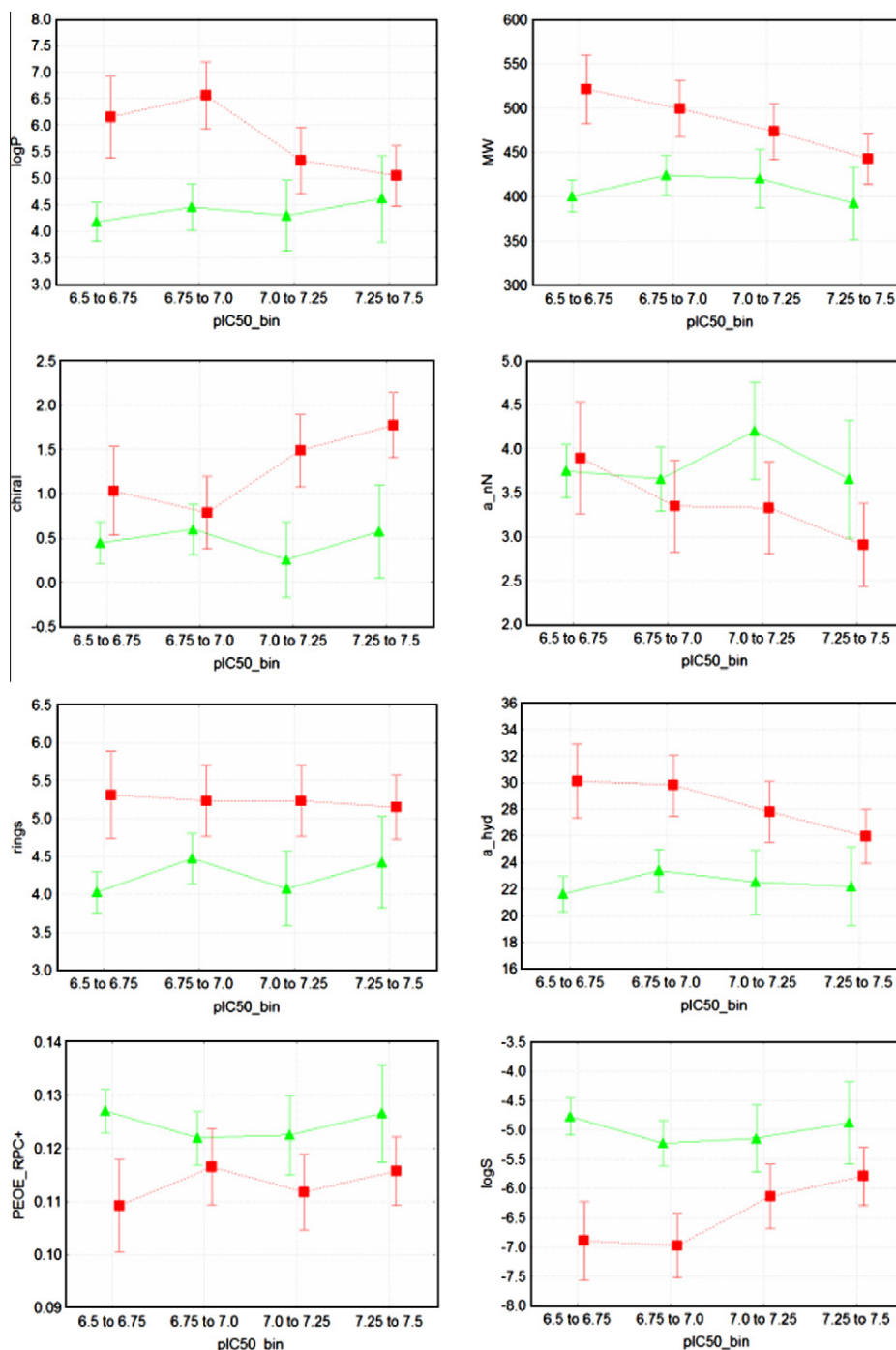


**Figure 9.** Relationship of selected descriptors (log *P*, MW, chiral, a<sub>nN</sub>, rings, a<sub>hyd</sub>, PEOE<sub>RPC+</sub>, log *S*) to fast (green) and slow (red) dissociation within ranges of affinity. The plots were derived via two-way ANOVA analysis and show the mean of each descriptor for the corresponding fast and slow classes of compounds, within each pIC<sub>50</sub> bin. The whiskers/bars indicate the 99.9% confidence level.

ligand.<sup>45,46</sup> Together, this is consistent with the hypothesis that fast and slow dissociating compounds may differ in their relative enthalpy and entropy of binding as revealed in this work by the difference between lipophilicity and size.

Research elsewhere has suggested that the fast dissociating properties of the dopamine stabiliser series represented by compounds ACR16, OSU6162 and NS30678, is due to their agonist like structural motif. In particular NS30678 showed D<sub>2</sub> affinity comparable to haloperidol yet was fast dissociating.<sup>25</sup> It is a commonly held perception that agonists of class A GPCRs tend to be smaller more hydrophilic molecules whereas antagonists are usually larger

and more lipophilic.<sup>26</sup> In their search for new antagonists the hydrophilic nature of the agonist starting point was preserved as opposed to following a conventional route of growing and adding lipophilicity. It was speculated that less lipophilic D<sub>2</sub> antagonists mimic the specific interactions of dopamine better than larger lipophilic antagonists. It is interesting that our analysis also highlights the important role of size, polarity and lipophilicity for fast dissociation.

In summary, analysis of a large dataset of D<sub>2</sub> receptor antagonists covering multiple chemical series with univariate and multivariate statistical approaches has identified that fast and slow

dissociating compounds can be discriminated based on their size, lipophilicity and polarity. Fast dissociating compounds are less lipophilic and have lower molecular weight. There is a tendency for them to have fewer rings and chiral centres and higher predicted log S. These data are in agreement with observations reported elsewhere based on the dopamine receptor stabiliser series. Although we can only speculate why this is the case the conclusions are nevertheless of value for the design of new antipsychotics acting at the D<sub>2</sub> receptor.

### Supplementary data

Supplementary data associated with this article can be found, in the online version, at [doi:10.1016/j.bmc.2011.02.033](https://doi.org/10.1016/j.bmc.2011.02.033).

### References and notes

- Marino, M. J.; Knutsen, L. J. S.; Williams, M. J. *Med. Chem.* **2008**, *51*, 1077.
- Van Rossum, J. M. In Brill, H., Cole, J., Deniker, P., Hippus, H., Bradley, P. B., Eds.; *Neuropsychopharmacology, Proceedings 5th Collegium Internationale Neuropsychopharmacologicum*; Excerpta Medica: Amsterdam, 1967; pp 321–329.
- Kapur, S.; Mamo, D. *Prog. Neuropsychopharmacol. Biol. Psychiatry* **2003**, *27*, 1081.
- Abi-Dargham, A.; Rodenhiser, J.; Printz, D.; Zea-Ponce, Y.; Gil, R.; Kegeles, L. S.; Weiss, R.; Cooper, T. B.; Mann, J. J.; Van Heertum, R. L.; Gorman, J. M.; Laruelle, M. *Proc. Natl. Acad. Sci.* **2000**, *97*, 8104.
- Seeman, P.; Chau-Wong, M.; Tedesco, J.; Wong, K. *Proc. Natl. Acad. Sci.* **1975**, *72*, 4376.
- Miyamoto, S.; Duncan, G. E.; Marx, C. E.; Lieberman, J. A. *Mol. Psychiatry* **2005**, *10*, 79.
- Tarsy, D.; Baldessarini, R. J. *Mov. Disord.* **2006**, *21*, 589.
- Leucht, S.; Pitschel-Walz, G.; Abraham, D.; Kissling, W. *Schizophr. Res.* **1999**, *35*, 51.
- Prolactin in Schizophrenia*; Peuskens, J., Ed.; Franklin Scientific Projects Ltd: London, 1997; pp 1–44.
- Waddington, J. L.; O'Callaghan, E. *CNS Drugs* **1997**, *7*, 341.
- Farah, A. J. *Clin. Psychiatry* **2005**, *7*, 268.
- Reynolds, G. P. *J. Psychopharmacol.* **1997**, *11*, 195.
- Perkins, D. O. *J. Clin. Psychiatry* **2002**, *63*, 1121.
- Weiden, P. J.; Mackell, J. A.; McDonnell, D. D. *Schizophr. Res.* **2004**, *66*, 51.
- Seeman, P. *Can. J. Psychiatry* **2002**, *47*, 27.
- Kawagoe, K. T.; Garriss, P. A.; Wiedemann, D. J.; Wightman, R. M. *Neuroscience* **1992**, *51*, 55.
- Koepp, M. J.; Gunn, R. N.; Lawrence, A. D.; Cunningham, V. J.; Dagher, A.; Jones, T.; Brooks, D. J.; Bench, C. J.; Grasby, P. M. *Nature* **1998**, *393*, 266.
- Cragg, S. J.; Rice, M. E. *Trends Neurosci.* **2004**, *27*, 270.
- Schultz, W. *Annu. Rev. Neurosci.* **2007**, *30*, 259.
- Copeland, R. A.; Pompliano, D. L.; Meek, T. D. *Nat. Rev. Drug Disc.* **2006**, *5*, 730.
- Tummino, P. J.; Copeland, R. A. *Biochemistry* **2008**, *47*, 5481.
- Lackey, K. *Curr. Top. Med. Chem.* **2006**, *6*, 435.
- Kapur, S.; Seeman, P. *J. Psychiatry Neurosci.* **2000**, *25*, 161.
- Natesan, S.; Svensson, K. A.; Reckless, G. E.; Nobrega, J. N.; Barlow, K. B. L.; Johansson, A. M.; Kapur, S. *J. Pharmacol. Exp. Ther.* **2006**, *318*, 810.
- Dyhring, T.; Nielsen, E. Ø.; Sonesson, C.; Pettersson, F.; Karlsson, J.; Svensson, P.; Christophersen, P.; Waters, N. *Eur. J. Pharmacol.* **2010**, *628*, 19.
- Pettersson, F.; Pontén, H.; Waters, N.; Waters, S.; Sonesson, C. *J. Med. Chem.* **2010**, *53*, 2510.
- (a) De Bruyn, M. F. L.; Macdonald, G. J.; Kennis, L. E. J.; Langlois, X. J. M.; Van den Keybus, F. A. M.; Van Roosbroeck, Y. E. M. PCT Int. Appl. WO 2007048779; *Chem. Abstr.* **2007**, *146*, 482080; (b) Macdonald, G. J.; Andrés-Gil, J. I.; Van den Keybus, F. A. M.; Bartolomé-Nebreda, J. M.; Van Gool, M. L. M. PCT Int. Appl. WO 2008068277; *Chem. Abstr.* **2008**, *149*, 54005; (c) Macdonald, G. J.; Bartolomé-Nebreda, J. M.; Van Gool, M. L. M. PCT Int. Appl. WO2008128996; *Chem. Abstr.* **2008**, *149*, 513833; (d) Macdonald, G. J.; Bartolomé-Nebreda, J. M.; Van Gool, M. L. M.; Delgado-Jiménez, F. PCT Int. Appl. WO 2008128994; *Chem. Abstr.* **2008**, *149*, 513698; (e) Macdonald, G. J.; Bartolomé-Nebreda, J. M. PCT Int. Appl. WO 2008128995; *Chem. Abstr.* **2008**, *149*, 513841.
- Leysen, J. E.; Gommeren, W. *J. Recept. Res.* **1984**, *4*, 817.
- Molecular Operating Environment, version 2008.10; Chemical Computing Group Inc.: 1255 University Street, Montreal, Quebec, Canada.
- ACD Labs software. pK<sub>a</sub>. Advanced chemistry development Inc. 110 Yonge Street, 14th Floor, Toronto, Ontario, Canada M5C 1T4. <http://www.acdlabs.com/home/>.
- Agrafiotis, D. K.; Simson, A.; Dai, H.; Derkinderen, A.; Farnum, M.; Gates, P.; Izrailev, S.; Jaeger, E. P.; Konstant, P.; Leung, A.; Lobanov, V.; Marichal, P.; Martin, D.; Rassokhin, D. N.; Shemanarev, M.; Skalkin, A.; Stong, J.; Tabruyn, T.; Vermeiren, M.; Wan, J.; Xu, X. Y.; Yao, X. *J. Chem. Inf. Model.* **2007**, *47*, 1999.
- STATISTICA 9.0, Statsoft Inc., 2300 East Tulsa, OK 74104, USA, <http://www.statsoft.com>.
- SIMCA-P 12, Umetrics, Tvistevägen 48, Box 7960, SE-907 19 Umeå, Sweden.
- Tropsha, A.; Golbraikh, A. *Curr. Pharm. Des.* **2007**, *13*, 3494.
- Gleeson, M. P. *J. Med. Chem.* **2008**, *51*, 817.
- Gleeson, M. P. *J. Med. Chem.* **2007**, *50*, 101.
- Liao, C.; Nicklaus, M. C. *J. Chem. Inf. Model.* **2009**, *49*, 2801.
- Bemis, G. W.; Murcko, M. A. *J. Med. Chem.* **1996**, *39*, 2887.
- Fernandez, J.; Alonso, J. M.; Andres, J. I.; Cid, J. M.; Diaz, A.; Iturrino, L.; Gil, P.; Megens, A.; Sipido, V. K.; Trabanco, A. A. *J. Med. Chem.* **2005**, *48*, 1709.
- Weaver, S.; Gleeson, M. P. *J. Mol. Graphics Modell.* **2008**, *26*, 1315.
- Wassvik, C. M.; Holmén, A. G.; Draheim, R.; Artursson, P.; Bergström, C. A. S. *J. Med. Chem.* **2008**, *51*, 3035.
- Lafont, V.; Armstrong, A. A.; Ohtaka, H.; Kiso, Y.; Amzel, L. M.; Freire, E. *Chem. Biol. Drug Des.* **2007**, *69*, 413.
- Freire, E. *Drug Discovery Today* **2008**, *13*, 869.
- Ferneczy, G. G.; Keserü, G. M. *J. Chem. Inf. Model.* **2010**, *50*, 1536.
- Kilpatrick, G. J.; El Tayar, N.; van de Waterbeemd, H.; Jenner, P.; Testa, B.; Marsden, C. D. *Mol. Pharmacol.* **1986**, *30*, 226.
- Borea, P. A.; Dalpiaz, A.; Varani, K.; Gilli, P.; Gilli, G. *Biochem. Pharmacol.* **2000**, *60*, 1549.